Current Control of a Multilevel Inverter based Matrix Converter

Gayatri Mohapatra

Abstract: ***An attempt is made to control the current of a PV integrated three-phase Cascaded H Bridge inverter, connected to a three-phase load with a matrix converter. The controller is designed to control the current and maintain the load power constant at any point of the disturbance enabling suitable control methods like PR controller {using the concept of inverter-current feedback (ICF)} and PI controller. A Matlab Simulink model of the said system is developed with suitable switching angles of the inverter switch selected using Differential Evolutional Algorithms (DEA). All the converters are modeled using a small scale averaging method to tune the controller. A novel controller technique of Matrix converter based multilevel inverter is proposed with the Proportional Resonant (PR) controller to control the power and the results are compared with the PI regulator. The ICF helps the PR controller to adjust the reference current and generate suitable control signal which is useful in reducing the harmonic content of the signal and hence a less distorted signal is produced during transients.***

Keywords: ***CHB-MLI, Matrix converter, Proportional Resonant controller, ICF, THD, DEA.***

I. INTRODUCTION

A Multilevel Inverter (MLI) is empowered to generate enormous power with a coordinated renewable energy sources having minimum dv/dt stress [1]. Power system optimization and a suitable range of the desirable controlling factors maintain a balance among the cost, power discrepancy and reliability with appropriate filtration methods. For power system estimation & grid integration, an optimum inverter design and power quality can be the constraints of trade-off. It is essential to evaluate the system performance, fidelity of the device and system prudential constraints when maintaining the power quality. In the field of cyclo converters, the matrix converters play a significant role in developing desired frequency output irrespective of the input. By employing the proper modulation technique, [10] the input-side power factor can be improved, which can eliminate the requirement of power factor correction devices at the cost of an increased number of switches. A tradeoff is always desirable when selecting control between the converter components and the conventional system. [14] The ripples generated due to switching frequencies needs to get the filter out with the help of the LCL filter. As the increased value of filter inductance provides high attenuation along with increased size of the filter [1, 3], it is preferred to implement control methods like (inverter-current feedback (ICF) or load-current feedback (LCF)) [8] to compensate for the low-order harmonics else a bulkier filter inductance can be a consequence. In ICF control the current sensors are accumulated in the inverter side for overcurrent surge and also supply an inherent damping characteristic to ensure the stability of the system under disturbed condition.

Many researchers have published articles to develop new concepts in these areas. Some of them are given below;

The THD reduction is justified by the increased number of levels in [1, 4] and by the comparison of the generation of delay angle by different modulation methods in [2]. A novel current feedback practice for PR control is proposed with a suitable weighted average value of the currents flowing through the feedback current regulator in [3]. The paper [5] minimizes the steady-state error of the grid currents injected in a series mode in the system. A functional switching model for conduction and switching losses in three-phase optimized harmonic stepped-waveform of MLI is developed in [6]. Multilevel Cascaded inverter with the different controllers like PI, PR, and Fuzzy is discussed in [7] for current control. The paper [8, 9] proposes a hybrid single carrier SPWM with a novelty of reduction in switching losses and improved harmonic performance for an inverter. A matrix converter is explained in topology, modulation scheme where look-up tables are avoided for modulation in [10, 11]. A new controller algorithm with a reactive power minimization is proposed in [12]. Fourier analysis of AC to AC converter is synthesized and a generalized transformation of the system is done in [13]. A PI and PR Controller are used for DC output voltage generation using the Space Vector Pulse Width Modulation Technique (SVPWM) in a three-phase Boost rectifier in [14]. A novel and simple control approach to controlling the power injection system (PIS) using state feedback is proposed in [16]. The paper [15, 17] presents a comparison of controller allowed in grid-connected PV to supply stable output with low total harmonic distortion (THD) as per standards under different grid loading conditions. The shortcomings of PI controllers in the form of steady-state error developed PR controllers with the practical application of PR current control for a photovoltaic (PV) inverter is also described in [18, 19]. A control based on the current as a variable for a Z source inverter is proposed in [20]. The Multi-step inverter with different topology is discussed with loss calculation and different carrier modulation methods in [21, 22]. The PR controller with a different variation of the control parameters is discussed in [23, 24] with photovoltaic control and adjustable speed control of ac drives.

Revised Manuscript Received on May 25, 2020.
***** Correspondence Author
Gayatri Mohapatra*, Department of Electrical Engineering, ITER, S'O'A (Deemed to be University), Bhubaneswar, India. Email: gayatrim79@gmail.com.

In this paper,

- A novel controller technique for the Matrix converter based Cascaded Inverter is proposed with proper tuning of the controller and modeling the same when connected to the three-phase load.
- The controller is customized to control the current with the PR controller and maintain the load power constant at any point of the disturbance, enabling suitable ICF by adjusting the current reference.
- Despite conventional PI regulator, the advantages of the PR controller for current control are discussed for different generated disturbances from the input as well as output side.
- The performances of the controllers are compared in the scale of Fast Fourier Transform (FFT) behavior, assuming constant PV system.

This article is organized by arranging Cascaded H- Bridge Multilevel inverter (CHB-MLI) in Section 2; System Modeling is done in 3. Matrix converter is in section 4 and the algorithm for Matrix converter in 5. Design of controller is in section 6, the System description and Problem Formulation in 7. waveform and results are shown in section 8 and finally, the conclusion is given in segment 9.

II. MULTILEVEL INVERTER (CHB_MLI)

The Inverter with a distinct level contains a cluster of power Silicon-based switches (IGBT) and capacitive voltage sources to skeleton an MLI. The switching sequel adds the strength of each bridge and finally, the output voltage is amplified at the endpoint, thereby reducing the resisting voltage of each switch. The CHB inverter has of an arrangement of single H_bridge units in series, hence accruing the least components as compared to other topologies and cost-effective. [15 and 16]

III. SYSTEM MODELLING

A. The Inverter output voltage Modelling

The voltage level per phase across the load of an MLI is explained by "(1)". [2, 6, 21]The delay to the switches is assigned to generate the demanded voltage and emit the minimum order harmonics which is the highest in magnitude among all the harmonic orders. The stretch of the load voltage U_{an} on the basis of Fourier's expansion is in "(2)". [4, 15, 21]

$$k=2s-1 \tag{1}$$

$$U_{an}(wt)=\sum_{x=1,3,5}^{\infty}\frac{4U_{dc}}{x\pi}\left[\begin{matrix}\cos ine(h\beta_1)\\ +.....+\cos ine(h\beta_s)\end{matrix}\right]\sin(hwt) \tag{2}$$

$$U_{an}=\sum_{z=1}^{s}U_{az} \tag{3}$$

$$h=3S-k_x,\quad k_x=1\therefore S=\text{even},\ k_x=2\therefore S=\text{odd} \tag{4}$$

$$\begin{matrix}\cos ine(\beta_1)+.....+\cos ine(\beta_S)=S\times M_m\\ .....\\ \cos ine(x\beta_1)+\cos ine(x\beta_3)+.....+\cos ine(x\beta_S)=0\end{matrix} \tag{5}$$

Inverter's steps number can be extracted from the "(2)" to achieve the optimal angle of switching, (β) of the load potential as in "(3)" with the expected bridge number as set in "(4)".The "(5)" can be used to extract the delay angle using DEA as an iterative technique. [5, 6, 7, 8, 9 and 21]

IV. MATRIX CONVERTER

The matrix converter as shown in Fig. 1 is a set of four-quadrant switches connected to three input legs to synthesize one output leg voltage. The common emitter four-quadrant switch configuration is used for simulation of the matrix converter [7, 11, and 15].

Output phases and input phases of the converters are represented as (A, B, C) and (a, b, c). The duty ratio of the three switches is set by a limit as in "(6)". The switching cycle average model of voltage and current of input and output phase voltage in terms of duty ratio is given in "(7)" and "(8)".

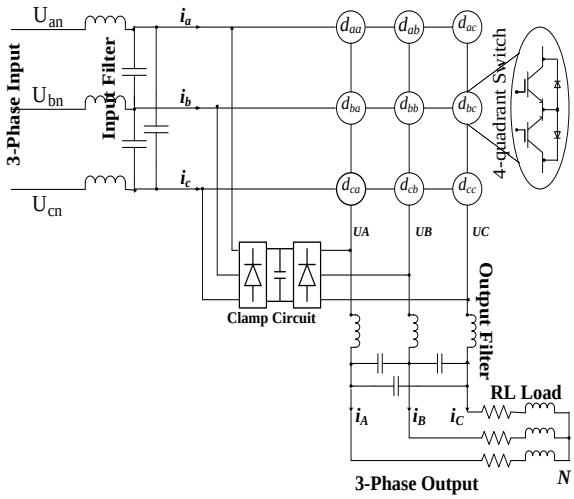

Figure.1 represents schematic diagram of Matrix converter

$$0\le(d_{ab},d_{bc},d_{ca})\le 1,\ d_{aa}+d_{ba}+d_{ca}=1 \tag{6}$$

$$\begin{bmatrix}U_{an}\ I_a\\ U_{bn},I_b\\ U_{cn}\ I_c\end{bmatrix}=\begin{bmatrix}d_{aa}&d_{ba}&d_{ca}\\ d_{ab}&d_{bb}&d_{cb}\\ d_{ac}&d_{bc}&d_{cc}\end{bmatrix}\begin{bmatrix}U_a\ I_a\\ U_b,I_b\\ U_c\ I_c\end{bmatrix} \tag{7}$$

$$\begin{aligned}U_a(t)&=d_{aa}U_{an}+d_{ba}U_{bn}+d_{ca}U_{cn}\\ U_b(t)&=d_{ab}U_{an}+d_{bb}U_{bn}+d_{cb}U_{cn}\\ U_c(t)&=d_{ac}U_{an}+d_{bc}U_{bn}+d_{cc}U_{cn}\end{aligned} \tag{8}$$

$$\begin{aligned}d_{aa}(t)&=k_a\sin(\omega_i(t))\\ d_{ba}(t)&=k_a\sin(\omega_i(t)-2\pi/3)\\ d_{ca}(t)&=k_a\sin(\omega_i(t)-4\pi/3)\end{aligned} \tag{9}$$

$$U_a(t)=\frac{3}{2}k_a(t)U_{in}\cos(\rho) \tag{10}$$

$$d_{aan} = d_{aa} + D_1 + D_4 - D_7 \quad (11)$$
$$d_{ban} = d_{ba} + D_2 + D_5 - D_8$$
$$d_{can} = d_{ca} + D_3 + D_6 - D_9$$

$$D_1(t) = \frac{1}{3} + \frac{1}{6}\left[\cos(3\omega_i t)\cos(\omega_i t)\right]$$
$$D_2(t) = \frac{1}{3} + \frac{1}{6}\left[\cos(3\omega_i t)\cos(\omega_i t + 2\pi/3)\right]$$
$$D_3(t) = \frac{1}{3} + \frac{1}{6}\left[\cos(3\omega_i t)\cos(\omega_i t + 4\pi/3)\right]$$
$$D_4(t) = \frac{-k_m}{6}\left[\cos(3\omega_o t)\cos(\omega_i t)\right]$$
$$D_5(t) = \frac{-k_m}{6}\left[\cos(3\omega_o t)\cos(\omega_i t + 2\pi/3)\right]$$
$$D_6(t) = \frac{-k_m}{6}\left[\cos(3\omega_o t)\cos(\omega_i t + 4\pi/3)\right]$$

$$D_7(t) = k_m \sin(3\omega_i t)\sin(\omega_i t)$$
$$D_8(t) = k_m \sin(3\omega_i t)\sin(\omega_i t + 2\pi/3)$$
$$D_9(t) = k_m \sin(3\omega_i t)\sin(\omega_i t + 4\pi/3)$$

Once the delay is set as per "(9)", the converter output voltage frequency which is independent of the input voltage frequency as derived in "(10)" is developed. [11] To synthesize maximum output magnitude on the output voltage the final duty ratios are developed in"(11)".

V. ALGORITHIM OF MATRIX CONVERTER

The algorithm proposed for the converter to achieve the required condition of delay is explained in Fig. 2.

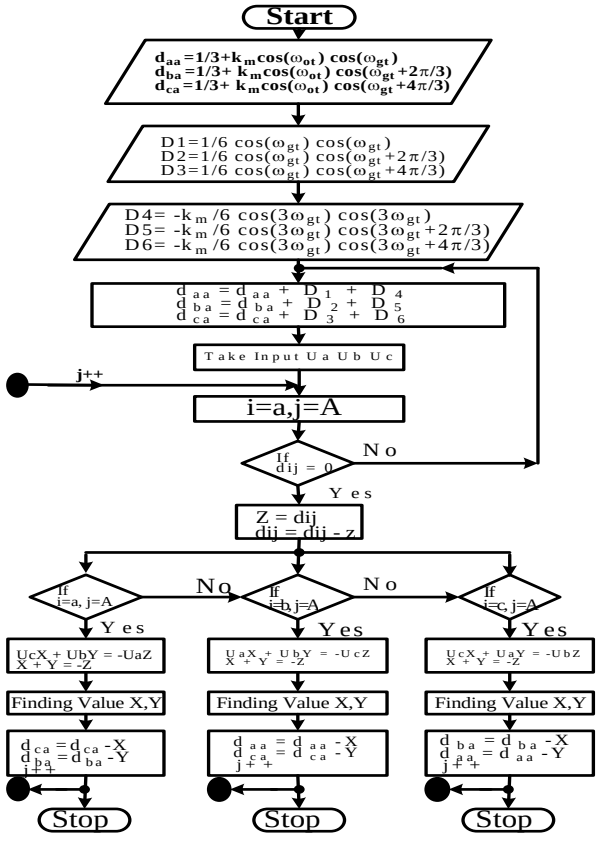

Figure.2 explains the complete Flow Chart of the proposed Algorithm

VI. CONTROLLER DESIGN

A. Proportional Resonant Controller (PR)

A Proportional Resonant (PR) is a controlling system with $H_c(s)$ the transfer function in "(12)" [15, 16, 23, and 24], which is equivalent to a PI controller in structure. The insertion of supplementary gain can enhance and regulate the frequency to make the system constraints to resonate at the required value. A compensator for harmonics reduction is given in "(13)" [9, 11]. G_h , can identify the frequencies close to the resonance without disturbing the spread of the controller. [10] This can be strongly applied in controlling the current with an advantage of synchronization of the current with the disturbances [17, 18, 19 and 20]. The final transfer function can be given in "(14)".

$$H_c(s) = K_{P1} + K_{I1}\frac{s}{s^2+\omega^2} \quad (12)$$

$$G_h = \sum_{h=3,5,7} K_{th}\frac{s}{s^2+(\omega h)^2} \quad (13)$$

$$G_{PR}(s) = \frac{2k_{p1}s+\chi_{p1}}{s^2+\omega_1^2} + \frac{2k_{p2}s+\chi_{p2}}{s^2+\omega_2^2} + \frac{2k_{p3}s+\chi_{p3}}{s^2+\omega_3^2} + \chi_{p4} \quad (14)$$

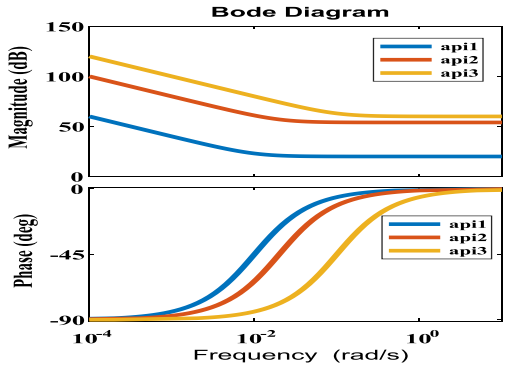

Figure.3 (a) explains the bode representation of the PI controller (api1<api2<api3)

From Fig. 3(a) and Fig.3 (b) it can be concluded that the PR controller has a better range of parameter variation due to a wide gain margin as compared to the PI controller.

The width of this frequency band (dependent upon the gain margin) depends on the value of proportional constant *Kp*. Smaller the value of *the constant of proportionality*, wider will be the band. The regulator can be tuned as per the demand depending upon different values of proportional constants.

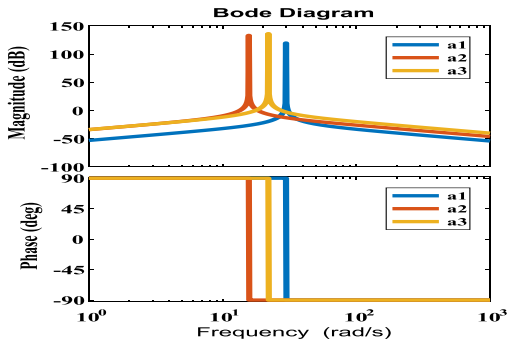

Figure.3 (b) explains the bode representation of the PR controller (a1<a2<a3)

B. Mathematical modeling of the system

The multilevel inverter can be modeled with respect to the switching sequence and the filter components as in "(15)" , "(16)" , "(17)" and "(18)" to tune the controller.

$$\frac{d}{dt}\begin{bmatrix} i_{ab} \\ i_{bc} \\ i_{ca} \end{bmatrix} = -\frac{r_L}{L}\begin{bmatrix} i_{ab} \\ i_{bc} \\ i_{ca} \end{bmatrix} - \frac{1}{3L}\begin{bmatrix} U_{ab} \\ U_{bc} \\ U_{ca} \end{bmatrix} + \frac{1}{3L}\begin{bmatrix} sw_a - sw_b \\ sw_b - sw_c \\ sw_c - sw_a \end{bmatrix} U_{dc} \tag{15}$$

$$\frac{d}{dt}\begin{bmatrix} U_{AB} \\ U_{BC} \\ U_{CA} \end{bmatrix} = -\frac{1}{RC_f}\begin{bmatrix} U_{ab} \\ U_{bc} \\ U_{ca} \end{bmatrix} + \frac{1}{C_f}\begin{bmatrix} i_{ab} \\ i_{bc} \\ i_{ca} \end{bmatrix} \tag{16}$$

$$\begin{bmatrix} \dot{X}_1 \\ \dot{X}_2 \\ \dot{X}_3 \\ \dot{X}_4 \\ \dot{X}_5 \\ \dot{X}_6 \\ \dot{X}_7 \\ \dot{X}_8 \\ \dot{X}_9 \\ \dot{X}_{10} \\ \dot{X}_{11} \\ \dot{X}_{12} \end{bmatrix} = \begin{bmatrix} -\frac{r_L+r_{cf}}{2L} & \omega & 0 & 0 & 0 & 0 & -\frac{1}{2L} & 0 & 0 & 0 & 0 & 0 \\ -\omega & -\frac{r_L+r_{cf}}{2L} & 0 & 0 & 0 & 0 & 0 & -\frac{1}{2L} & 0 & 0 & 0 & 0 \\ 0 & 0 & -\frac{r_L+r_{cf}}{2L} & \omega & 0 & 0 & 0 & 0 & -\frac{1}{2L} & 0 & 0 & 0 \\ 0 & 0 & -\omega & -\frac{r_L+r_{cf}}{2L} & 0 & 0 & 0 & 0 & 0 & -\frac{1}{2L} & 0 & 0 \\ 0 & 0 & 0 & 0 & -\frac{r_L+r_{cf}}{2L} & \omega & 0 & 0 & 0 & 0 & -\frac{1}{2L} & 0 \\ 0 & 0 & 0 & 0 & -\omega & -\frac{r_L+r_{cf}}{2L} & 0 & 0 & 0 & 0 & 0 & -\frac{1}{2L} \\ \frac{1}{C} & 0 & 0 & 0 & 0 & 0 & -\frac{r_L+r_{cf}}{2L} & \omega & 0 & 0 & 0 & 0 \\ 0 & \frac{1}{C} & 0 & 0 & 0 & 0 & -\omega & -\frac{r_L+r_{cf}}{2L} & 0 & 0 & 0 & 0 \\ 0 & 0 & \frac{1}{C} & 0 & 0 & 0 & 0 & 0 & -\frac{r_L+r_{cf}}{2L} & \omega & 0 & 0 \\ 0 & 0 & 0 & \frac{1}{C} & 0 & 0 & 0 & 0 & -\omega & -\frac{r_L+r_{cf}}{2L} & 0 & 0 \\ 0 & 0 & 0 & 0 & \frac{1}{C} & 0 & 0 & 0 & 0 & 0 & -\frac{r_L+r_{cf}}{2L} & \omega \\ 0 & 0 & 0 & 0 & 0 & \frac{1}{C} & 0 & 0 & 0 & 0 & -\omega & -\frac{r_L+r_{cf}}{2L} \end{bmatrix} \begin{bmatrix} x_1 \\ x_2 \\ x_3 \\ x_4 \\ x_5 \\ x_6 \\ x_7 \\ x_8 \\ x_9 \\ x_{10} \\ x_{11} \\ x_{12} \end{bmatrix} + \begin{bmatrix} \frac{\sqrt{3}mv_{dc}\cos(\varphi_a - \frac{\pi}{6})}{12L} \\ \frac{-\sqrt{3}mv_{dc}\cos(\varphi_a - \frac{\pi}{6})}{12L} \\ \frac{\sqrt{3}mv_{dc}\cos(\varphi_b - \frac{\pi}{6})}{12L} \\ \frac{-\sqrt{3}mv_{dc}\cos(\varphi_b - \frac{\pi}{6})}{12L} \\ \frac{\sqrt{3}mv_{dc}\cos(\varphi_c - \frac{\pi}{6})}{12L} \\ \frac{-\sqrt{3}mv_{dc}\cos(\varphi_c - \frac{\pi}{6})}{12L} \\ 0 \\ 0 \\ 0 \\ 0 \\ 0 \\ 0 \end{bmatrix} \tag{17}$$

$$x_1 = i_{ab}, x_2 = ji_{ab}, x_3 = i_{bc}, x_4 = ji_{bc}, x_5 = i_{ca}, x_6 = ji_{ca}, x_7 = U_{ab}, x_8 = jU_{ab}, x_9 = U_{bc}, x_{10} = jU_{bc}, x_{11} = U_{ca}, x_{12} = jU_{ca} \tag{18}$$

C. Modeling of the filter

The filter parameters of a LC filter can be designed as given in "(19)" and "(20)".

$$G_F(s) = R_f + \frac{s^2 L_{f1} C_f + 1}{s^3 L_{f1} L_{f2} C_f + s(L_{f1} + L_{f2})} \tag{19}$$

$$L_f \frac{di}{dt} = U_{dc}, L_f = \frac{U_{dc}}{\Delta I^* m_i * f_{sw}}, \tag{20}$$

$$C_f = \frac{15\%(MVAR)}{2 * \pi * f_{sw} * U^2}, R_f = 2\xi\sqrt{\frac{L_f}{C_f}}$$

D. PR Controller operating in model

The complete PR controller, as given in Fig. 4 takes the set controller parameters with suitable tuning which can be done by linearizing the total system. The combination blocks for the PR controller and complete ICF given in Fig. 5 (a), Fig. 5 (b) and Fig. 5 (c). The final block diagram of a PV integrated three phases MLI with a Matrix converter is shown in Fig. 6.

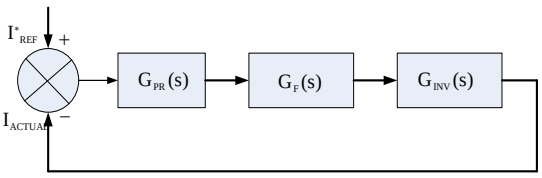

Figure.4 explains the overall system arrangement to control the load current using PR regulator with respect to transfer function

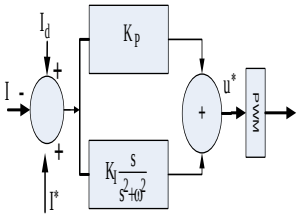

Figure.5 (a) Block diagram of PR regulator

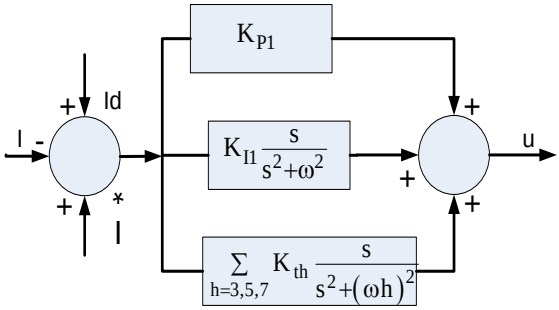

Figure.5 (b) Block diagram of PR regulator with Harmonic content

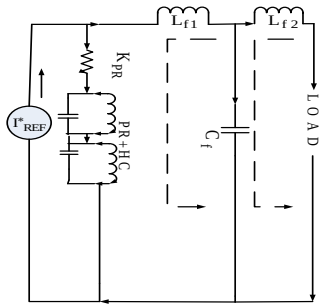

Figure.5 (c) Block diagram of ICF regulator with PR Regulator

Figure.5 explains the overall system arrangement to control the load current using PR regulator

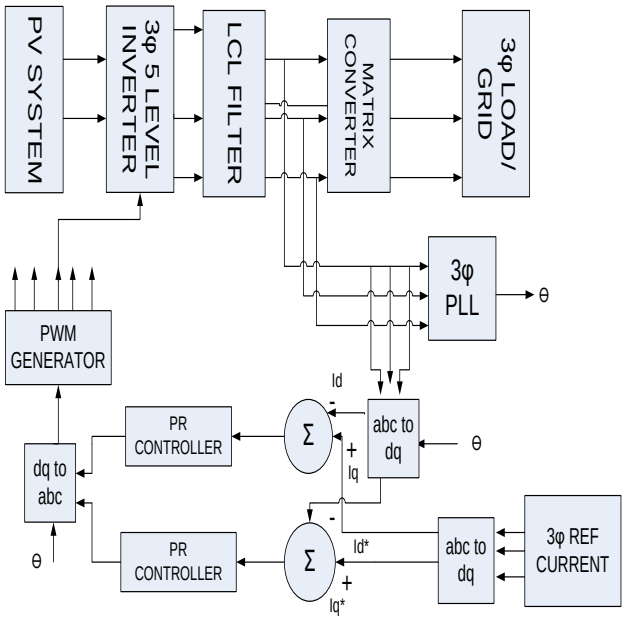

Figure.6 explains the overall system arrangement to control the load current using PR regulator

VII. SYSTEM DESCRIPTION AND PROBLEM FORMULATION OF PROBLEM

The proposed system aims in implementing the ICF method in regulating the load current within the range during the disturbance caused from the voltage harmonics distortions (due to the injection of the harmonic current is circulated freely through the filter capacitors present in the inverter as well as matrix converter side) and the load variation. This can be achieved by dragging the inverter current is to zero by a PR controller and resonant harmonic controllers (HCs).

The key point to enable control is to generate a reference current (I*) with the information of the harmonic content that can be realized by calculating the capacitor current from the capacitor voltage and then adding it into the reference. The description about the ICF is given in Fig.5 (c). This idea has been incorporated effectively for the ICF control system with a basic objective to get effectuated in the process of integration and achieve low THD.

A three phase five level CHB Inverter is designed in Matlab Simulink environment with the cascaded Matrix converter. The DEA is used to calculate the optimized delay angle as per the predefined objective function as in "(5)". The disturbances in the form of PV amplitude change and torque change are introduced and the ICF based PR controller and PI controller are used to find out the Stability.

The detail controller diagram and the system block diagrams are given in section VII.

Assuming each PV generator operating at its MPP, and the load voltage is a function of optimum delay angle, the current in the load side must maintain stability for any generated disturbance. Power factor correction can be achieved with the matrix converter in the input side of the inverter operating with variable frequencies. The total model is operated at a switching frequency of 10 kHz.

VIII. SIMULATION AND RESULT ANALYSIS

A Matlab Simulink model is developed and the controller is designed in accordance with the block diagram as shown in Fig. 6 with the forethought of the reasonable angle of delaying of MLI and switching sequence of Matrix converter with the parameters of simulation assigned as in Table 1.

TABLE 1
Parameters assigned for simulation

System Parameter	
PV voltage	70V
Matrix output voltage	120V
Load voltage	100V
Reference current set	5A
Load current	<5A
Matrix converter Parameter	
Km,Km1, ρ	0-0.57,0-0.22,0.5-1
Input filter	6mH,1micro F
Output filter	3mH,10 micro F
PR Regulator	
Kpn, χ_P	0-0.5,0-100
Filter for Inverter	
Input filter	1mH,10micro F
Output filter	5mH,10 micro F

Motor Specification Three phase Squirrel Cage Induction Motor	
Nominal Power	300Watt
Lime voltage	100V
Frequency	50Hz
Stator Resistance and Inductance	16.6 ohm,0.0131H
Rotor Resistance and Inductance	15.3 ohm,0.0131H
Mutual Inductance	0.825H
Friction factor	0.001
Pole pair , Inertia	4 ,0.05kg.m^2

A. Simulation waveform and result analysis

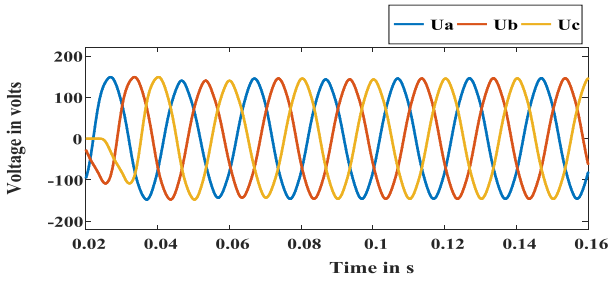

Figure.7 gives the inverter output voltage after filter

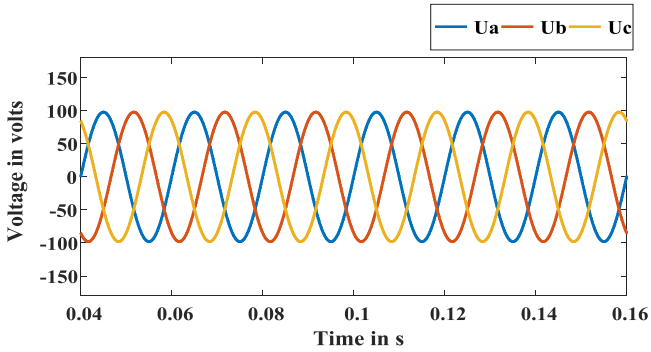

Figure.8 gives the matrix converter output voltage

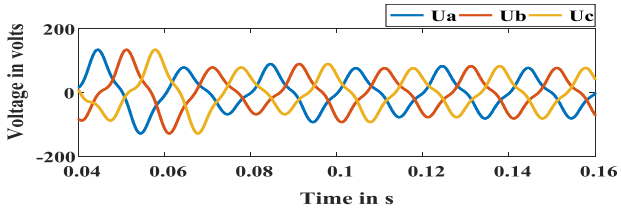

Figure.9 gives the Load voltage with PR controller

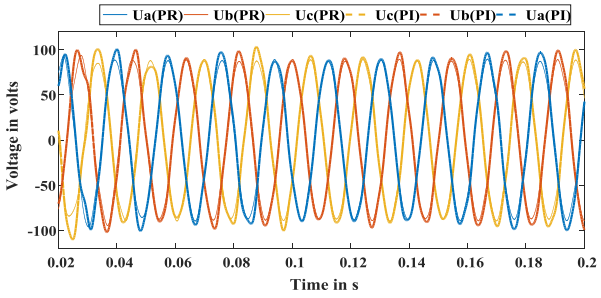

Figure.10 gives the Load voltage with the change of frequency with different controller

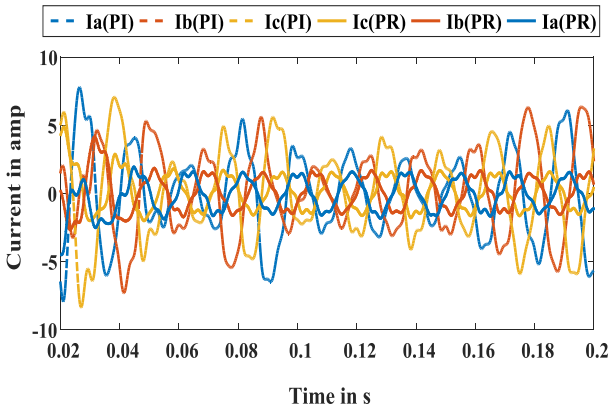

Figure.11 gives the Load current with the change of frequency with different controller

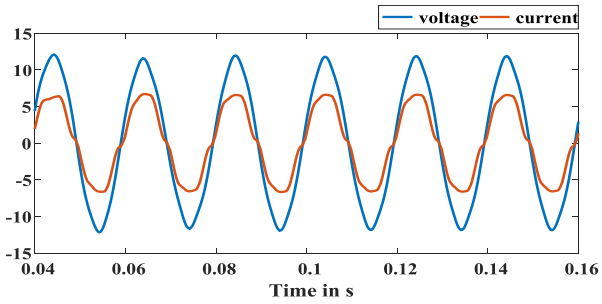

Figure.12 gives the matrix converter input voltage and current showing power factor improvement where the voltage is scaled down to 12percent with filter.

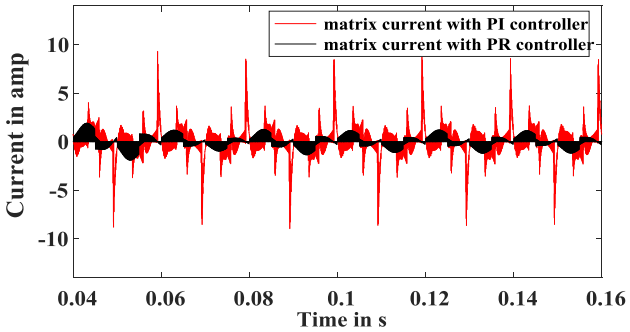

Figure.13 gives the matrix converter current with PI and PR controller.

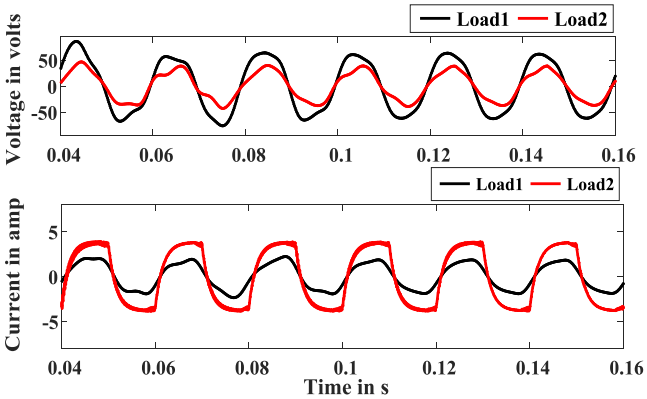

Figure.14 gives the Load voltage and current of the system with PR controller with different loads

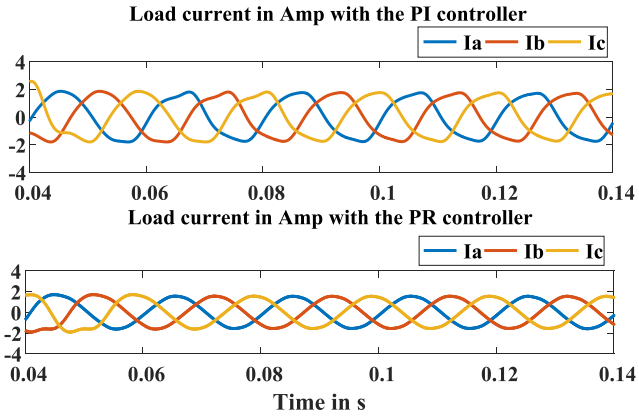

Figure.15 explains the Load current of the system with PI and PR controller with the voltage sag.

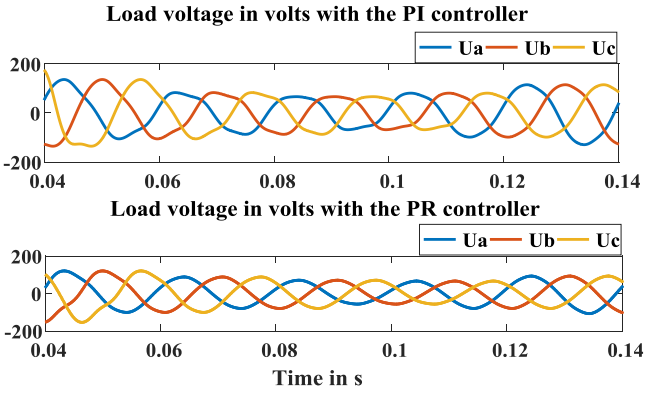

Figure.16 explains the Load voltage of the system with PI and PR controller with voltage sag.

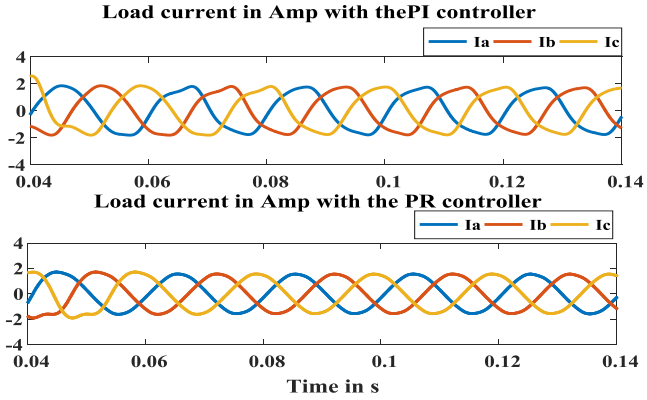

Figure.17 explains the Load current of the system with PI and PR controller.

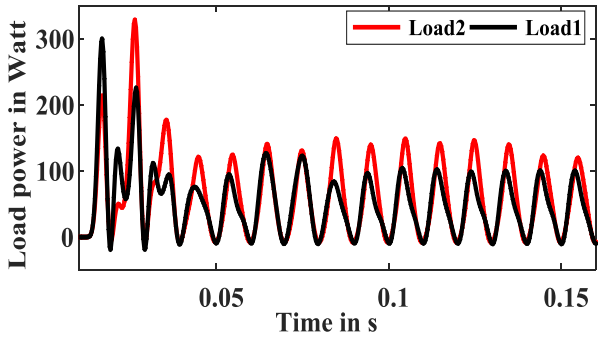

Figure.18 explains the Load power of the system with PR controller with different loads

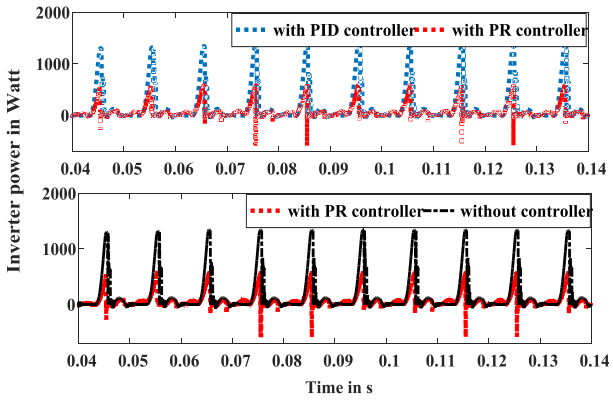

Figure.19 explains Inverter power of the system with and without controller and with different controllers

The load currents for load variation and input voltage disturbances in the form of PV amplitude change are imported to investigate the attitude of the controller and the responses are presented. The waveforms obtained from simulation are as shown above .They can be summarized to the following points of observations;

1. The simulated output voltage of the inverter per phase as in Fig. 7 after the filter is allowed to pass through the Matrix converter with the calculated filter parameter to give the output voltage of the matrix converter in Fig.8 and Load voltage in Fig.9.
2. The change of frequency is incorporated as a deviation from the set value and the response with different controllers is observed in Fig.10 and Fig.11 in the form of voltage and current signals respectively to justify the superiority of the PR controller.
3. Fig.12 gives a required power factor improvement of the matrix converter when the voltage is scaled down to match the current scale.
4. The matrix converter waveform showing the output current contains lesser spikes with the PR controller in Fig.13 as compared to the PI controller.
5. The three phase load current is varied with the load change in the form of torque variation of the three phase induction motor. The response with the PI and the PR controller is given in Fig.14. From the same figure the smoothness with the PR controller is validated.
6. Voltage sag of 0.8pu is inserted from the input side for a time interval of [0.06s to 0.12s] and response of the system is analyzed with the PR and PI controller. With the insertion of disturbance from the PV side for the interval of [0.06s to 0.12s] in the form of the voltage sag, the voltage and current are showing the comparison with and without the controller in Fig. 15 and Fig. 16.
7. The load current without sag and for a load variation in the form of torque is given in Fig. 17.
8. The load power response is explained in Fig.18 and 19 for different loading using the PR controller and the spikes are reduced with the PR controller.
9. The FFT analysis of the load current is explained in Table 2.From that it is obvious that the PR controller is better in reducing the harmonic.

Table2
FFT list of different harmonic content with different controller

	5^{th}		7^{th}		9^{th}		11^{th}	
	PI	**PR**	**PI**	**PR**	**PI**	**PR**	**PI**	**PR**
Fundamental	5.5	4.9	5.1	4.23	4.8	3.9	2.2	1.9
Fundamental with 5^{th} compensated	1.1	0.35	4.2	3.85	3.1	2.2	1.5	1.4
Fundamental with 5^{th} ,7^{th} compensated	2.3	0.44	0.5	0.86	2.36	2.4	0.5	0.9
Fundamental with 5^{th} ,7^{th} ,9^{th} compensated	1.9	0.37	2.1	0.61	0.43	0.24	0.49	0.4
Fundamental with 5^{th} ,7^{th} ,9^{th} ,11^{th} compensated	0.5	0.28	0.28	0.39	0.16	0.21	0.1	0.1

IX. CONCLUSION

A new current control technique using the concept of ICF is applied in a five-level three-phase CHB multilevel inverter connected to a three phase squirrel cage induction motor load with a matrix converter with the PV system as input. In spite of the limitation of low voltage regulation in the matrix converter, the improved power factor and the naturally commutated ac to ac converter structure dominates the use of the same in the system. The observations made from the simulated waveforms and the analysis obtained from the FFT amplitude can prove the superiority of the PR controller on the PID regulator. The ICF method can able to control the load current within the reference value with appreciable THD reduction is also justified.

The design of the filter can be set for more accurate values to reduce the harmonic percentage in the load voltage waveforms and also controller design from the matrix converter side can be considered to be the future scope.

Nomenclature

β	Optimal angle of switching
k_{vgain}	Output voltage gain (maximum).
β_1–β_s	The angles of switching of the IGBT
G_h	The compensator harmonic transfer function
ξ	The filter coefficient
L_f , C_f , R_f	The filter inductance, capacitance and resistance
D_1–D_7	The final delay angles of Matrix converter
K_{th} , K_{PI}, K_{II}	The gain of the compensator.
χ_{P1}, k_{p1}	The gain of the compensator.
Km, km1	The improvement constants
M_m	The index required for modulation
U_{az}	The individual source voltage for S number of sources
U_{an}	The Inverter phase voltage
R , L	The load components
r_L , r_{cf}	The lumped parameters of filter inductance and capacitance
$U_a(t)$	The matrix output voltage in time variant representation
S	The number of H Bridge of the inverter
h	The number of order of harmonic
ρ	The offset duty ratio correction factor
$G_{PR}(s)$	The overall Controller transfer function
I_a	The phase current
I^*	The Reference current
d_{aa}	The switching delay of the first switch first arm of the converter
f_{sw}	The switching frequency
$H_c(s)$	The transfer function of PR controller
$G_F(s)$	The transfer function of the filter
U_{dc}	Voltage of the dc capacitor

REFERENCES

1. Rodriguez, Jose, Jih-Sheng Lai, and Fang Zheng Peng, "Multilevel inverters: a survey of topologies, controls, and applications". *IEEE Transactions on industrial electronics* 49.4 (2002), 724-738.
2. Yao, Wenxi, Haibing Hu, and Zhengyu Lu, "Comparisons of space-vector modulation and carrier-based modulation of multilevel inverter". *IEEE transactions on Power Electronics*23.1 (2008), 45-51.
3. Shen, Guoqiao, et al. "A new feedback method for PR current control of LCL-filter-based grid-connected inverter". *IEEE Transactions on Industrial Electronics* 57.6 (2010): 2033-2041.
4. Mittal, Nupur, et al. Multilevel inverters: "A literature survey on topologies and control strategies. 2012 *2nd International Conference on Power, Control and Embedded Systems". IEEE*, 2012.
5. Nirmal, S., et al. "Steady state error elimination and harmonic compensation using proportional resonant current controller in grid-tied DC microgrids".2018 *International Conference on Power, Instrumentation, Control and Computing (PICC).* IEEE, 2018.
6. Aghdam, M. Ghasem Hosseini, S. Hamid Fathi, and Azadeh Ghasemi. "The analysis of conduction and switching losses in three-phase OHSW multilevel inverter using switching functions". *2005 International Conference on Power Electronics and Drives Systems. Vol. 1. IEEE*, 2005.
7. Dey AK, Mohapatra G, Mohapatra TK, Sharma R. "A Modified Venturini PWM scheme for Matrix converters". In *2019 IEEE International Conference on Sustainable Energy Technologies (ICSET)* (pp. 013-018). IEEE.
8. Mohapatra, Gayatri, Asim Kumar Dey, and Renu Sharma. "Comparison of controller in a three phase CHB Inverter".*2019 IEEE International Conference on Sustainable Energy Technologies (ICSET).* IEEE.
9. Govindaraju, C., and K. Baskaran. "Performance improvement of multiphase multilevel inverter using hybrid carrier based space vector modulation". *International Journal on Electrical Engineering and Informatics 2.2 (2010)*: 137-149.
10. Mohapatra, K. K., et al. "A novel carrier-based PWM scheme for matrix converters that is easy to implement".2005 *IEEE 36th Power Electronics Specialists Conference. IEEE, 2005.*
11. Alesina, Alberto, and Marco GB Venturini. "Analysis and design of optimum-amplitude nine-switch direct AC-AC converters". *IEEE Transactions on Power Electronics 4.1* (1989): 101-112.
12. Venturini, Marco, and Alberto Alesina. "The generalized transformer: A new bidirectional, sinusoidal waveform frequency converter with continuously adjustable input power factor".1980 *IEEE Power Electronics Specialists Conference. IEEE,* 1980.
13. Alesina, Alberto, and M. Venturini. Solid-state power conversion: "A Fourier analysis approach to generalized transformer synthesis". *IEEE transactions on circuits and systems 28.4* (1981): 319-330.

14. Gnanavadivel, J., et al. “Performance Analysis of PI Controller and PR Controller Based Three-Phase AC-DC Boost Converter with Space Vector PWM”. *International Journal of Pure and Applied Mathematics 118.24* (2018): 1-16.
15. Mohapatra, Gayatri. “Current control of a PV integrated CHB-multilevel inverter using PR controller”.*2018 Technologies for Smart-City Energy Security and Power (ICSESP). IEEE,* 2018.
16. Mohapatra, Gayatri, and Asim Kumar Dey. "Current Control of a CHB Multilevel Inverter Using PR and Adaptive Fuzzy PI Controller: A Comparison." *Advanced Computing and Intelligent Engineering*. Springer, Singapore, 2020. 11-21.
17. Arul Kumar, K.D. Vijayakumar, and K. Palanisamy. “Modeling and control strategy of three phase neutral point clamped multilevel PV inverter connected to the grid”. *Journal of Building Engineering 3 (2015):* 195-202.
18. Teodorescu, Remus, Frede Blaabjerg, and Marco Liserre. “Proportional-resonant controllers. A new breed of controllers suitable for grid-connected voltage-source converters”. *Proc. Optimum 3 (2004),* 9-14.
19. Komurcugil, Hasan, et al. “Model-based current control for single-phase grid-tied quasi-Z-source inverters with virtual time constant” .*IEEE Transactions on Industrial Electronics 65.10* (2018): 8277-8286.
20. Escobar, Gerardo, et al. “Design of an inverter-side current reference and controller for a single-phase LCL-based grid-connected inverter”. *International Transactions on Electrical Energy Systems 28.1 (2018)*: e2476.
21. Mohapatra, Gayatri, and Manas Ranjan Nayak. “Switching Angle and Power Loss Calculation for THD Minimization in CHB-Multilevel Inverter Using DEA”. *Information and Decision Sciences*. *Springer, Singapore, 2018*. 491-502.
22. Reddy, C. Lokeshwar, P. Satish Kumar, and M. Sushama. Design and “Performance Analysis of 7-Level Diode Clamped Multilevel Inverter Using Modified Space Vector Pulse Width Modulation Techniques”. *International Journal of Engineering-Transactions B: Applications 30.11 (2017):* 1762-1770.
23. Zammit, Daniel, et al. “Design of PR current control with selective harmonic compensators using Matlab”. *Journal of Electrical Systems and Information Technology 4.3 (2017):* 347-358.
24. Matteini, Marco. “Control techniques for matrix converter adjustable speed drives”. *Diss. Ph. D. Dissertation, Dept. Electrical. Eng., Univ. Bologna, Bologna, Italy, 2001*.

AUTHORS PROFILE

Gayatri Mohapatra received her BE degree from ITER Bhubaneswar in Electrical Engineering. She has completed MTech in power electronics from RVCE Bangalore in the year 2011 and recently working as an Assistant Professor, Electrical Engineering Dept. of ITER, SOA University, Bhubaneswar, and Odisha, India. Her area of interest are Power electronics based drives and controller design. She is also interested in adaptive fuzzy logic based controllers for inverter based drives.